ELSEVIER

*Applied Acoustics* **45** (1995) 227–245

0003-682X/95/$9.50

0003-682X(94)00047-6

# Calculation of the Mean and Maximum Mobility for Concrete Floors

A. T. Moorhouse & B. M. Gibbs

School of Architecture and Building Engineering, University of Liverpool, Liverpool, UK, L69 3BX

(Received 13 January 1994; revised version received 21 November 1994; accepted 6 December 1994)

*ABSTRACT*

*When calculating the structure-borne sound power of a vibration source, such as machines or footfall, it is necessary to know the point mobility of the supporting floor. The frequency-averaged mobility is easily calculated, but the height of the resonant peaks is also important for power flow at low frequencies. This paper describes how the complicated mobility curve for rods, beams and plates can be reduced to a skeleton plot consisting of a mean line, and an envelope of the resonant peaks. Skudrzyk's 'mean value method'[1] is used to provide a simple expression for the peak envelope which is independent of the resonance frequencies. The formula is exact for rods and beams when coupling losses are correctly included. For plates a good approximation is obtained and the predicted skeleton plot shows good agreement with measured mobilities of concrete floors.*

## 1 INTRODUCTION

The objective of this paper is to develop a simple characterisation of the mobility curve for concrete floors which will provide an engineering feel for the problem with a minimum of complication. The intended application is to calculation of the transmitted structure-borne sound power from machines into their supporting floor.[2,3,4] (Mobility is the complex ratio of velocity to applied force at a point, i.e. the inverse of mechanical impedance.)

It is well known that the mobility of continuous elements, such as beams and plates, converges to the characteristic mobility at high frequencies where many resonances overlap. At lower frequencies, where

resonances are separated, resonance peaks and antiresonance troughs extend respectively above and below the characteristic line[5] (see Figs 1 and 2 for example). For excitation by tonal sources such as machines, the actual value of mobility at the excitation frequency is of importance, not just the frequency-averaged value. However, detailed calculation of the mobility curve in the resonant range is usually impractical because the behaviour is complicated. A simplified characterisation consisting of a mean line, and an envelope to include the resonant peaks is therefore proposed (Fig. 1).

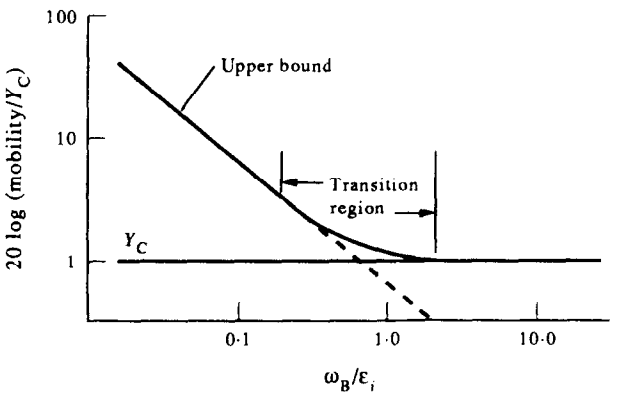


**Fig. 1.** Skeleton mobility plot showing mean and peak envelope.

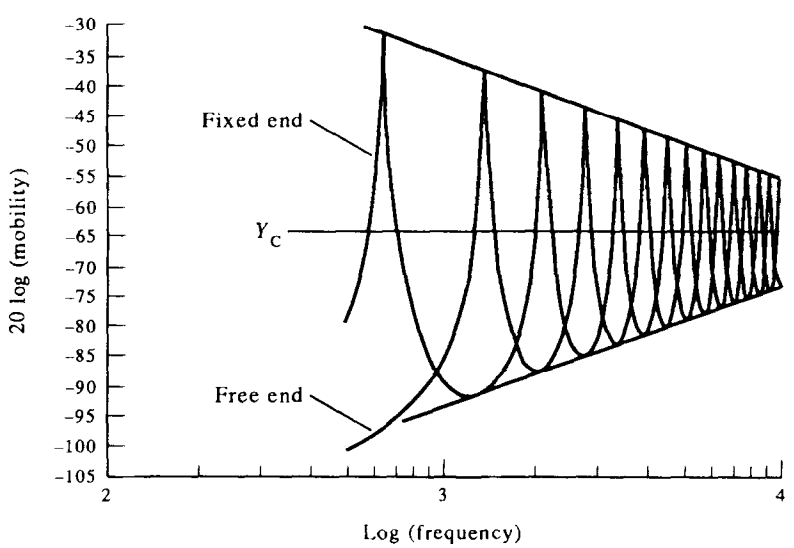


**Fig. 2.** Point mobility of end-excited rods with clamped and free ends.

Several authors have obtained estimates for the heights of the resonance peaks of concrete floors, mostly empirically and with little or no theoretical support.[6,7,8] Steel[9] has suggested a method of analysis based on the decomposition of plate response into single modes but a more general method will now be investigated.

The 'mean value method', from Skudrzyk,[1,10] has been shown by Williams[11] to be successful in predicting the mean mobility of freely suspended metal plates, and a prediction of the height of the resonances has yielded promising agreement with measurement. This theory will be briefly reviewed and application to building elements examined by means of illustrative examples on simple theoretical models and a limited number of real floors.

## 2 THEORY

Skudrzyk[1] expresses the characteristic mobility for any continuous element in terms of the average modal spacing $\epsilon_i$ and the so called modal mass $M_i$ as:

$$\mathrm{Re}\,[\bar{Y}_c] = \frac{\pi}{2}\,\frac{1}{M_i \epsilon_i} \tag{1}$$

The resonant peaks and antiresonant troughs are respectively a factor $\beta$ above and below the characteristic mobility where:

$$\beta = \frac{2}{\pi}\,\frac{\epsilon_i}{\omega_B} \tag{2}$$

in which $\omega_B = \omega_i \cdot \eta$ is the modal bandwidth of a resonance at $\omega_i$ with $\eta$ the total loss factor. The resonant peaks are of most interest since this constitutes the worst case in terms of the power absorbed by the structure, and by combining eqns (1) and (2) the mobility at a resonance peak is:

$$Y_r = \mathrm{Re}\,[\bar{Y}_c] \cdot \beta = \frac{1}{M_i \omega_B} \tag{3}$$

This is real by definition at a resonance. $M_i$ is half the total mass of the element for one-dimensional modes such as occur in rods and beams, and for quasi-beam modes in plates; for two-dimensional plate modes the fraction is $\frac{1}{4}$.[1]

An envelope for the resonance peaks can now be drawn without knowledge of the resonance frequencies $\omega_i$. The limit line, which indicates the height a resonance would attain if it occurred at $\omega$, say, is given by:

$$Y_r = \frac{2}{M \cdot \omega \cdot \eta} \qquad \text{for rods and beams} \tag{4}$$

$$Y_r = \frac{4}{M \cdot \omega \cdot \eta} \qquad \text{for plates} \tag{5}$$

The above assumes the response to be dominated by a single mode. When allowing for modal overlap, Williams[11] gives the height of the peaks as:

$$Y_r = \mathrm{Re}\,[\bar{Y}_c] \cdot \mathrm{cotanh}\,(1/\beta) \tag{6}$$

Equation (6) reduces to eqn (3) at low frequency and to the characteristic value at high frequency. Figure 1 shows the relative heights of the peaks above the characteristic mobility and is general for rods, beams, plates and shells. Thus, the required characterisation, namely the mean and the peak envelope, can be obtained using simple formulae, eqns (4), (5) and (6).

In general, when structural elements are subject to excitation the position of excitation and the boundary conditions have a strong influence on the mobility curve. It is remarkable then that equations (5) and (6) indicate that there is no dependence of the peak envelope on either of these factors (except in so far as the boundary conditions affect loss factor). This far-reaching result will first be investigated using exact solutions for simple systems of rods, beams and plates, before the formulae are applied to real concrete floors.

## 3 THE EFFECT OF BOUNDARY CONDITIONS AND EXCITATION POSITION

Mobilities of two rods with fixed and free ends are shown in Fig. 2. The natural frequencies are different for each configuration, yet eqn (4) exactly predicts the resonant peaks for both cases. Exact agreement is also obtained for beams with simply supported, clamped, and free boundary conditions with the exception of the lowest resonance for which end distortion causes a small discrepancy. Therefore, for rods and beams, the peak envelope is independent of the boundary conditions (assumed to be lossless at this stage).

Turning attention now to the effect of excitation position, the mobility of a rod with fixed ends is shown in Fig. 3. The variation in mobility with increased distance of the excitation point from the centre is illustrated. Excitation at the centre causes antisymmetric modes to be excited to their full height, and their peaks touch the predicted upper limit. Away from the centre some modes are partially excited and the prediction is conservative. The mobility at the boundary is theoretically zero, and in practice would be small.[12] Equation (4) is therefore applicable for rods excited at any position. Prediction is exact if the excitation coincides with an antinode, and conservative for other positions. There is no reason to suppose that this conclusion does not hold for beams.

The situation for plates is more complicated as illustrated in Fig. 4 where the mobility of a simply supported plate is plotted for various aspect ratios (for this example $M = 39$ kg and $\eta = 5\%$) The results indicate an important difference from rods and beams, which are one-dimensional wave guides and have regularly spaced resonances, (see Fig. 2, where for rods the modal spacing is constant). For plates, the *average* modal spacing is frequency invariant[13] but it is possible for modes to bunch together. Thus it is possible for, say, two coincident resonances to double the response, but only if both are simultaneously excited at an antinode. The worst case for such increases in response is for square plates excited at the centre, as shown in Fig. 4, because square plates have several coincident resonances, and the centre is always an antinode for symmetrical modes. For non-square plates, exactly coincident resonances are less likely, and for non-central excitation the chance of full excitation of all modes is reduced. These trends are illustrated in Fig 4. Thus, eqns (5) and 6) will yield reasonable estimates of peak height for plates with any (lossless) boundary conditions, although not a strict upper bound.

## 4 THE EFFECT OF COUPLING LOSSES

In the examples so far, only material losses have been present. In theory one can also include coupling losses by use of the total loss factor:

$$\eta = \eta_m + \eta_c \tag{7}$$

in which $\eta_c$, and $\eta_m$ are the coupling and material loss factors respectively. An example will illustrate whether this is possible in practice.

Figure 5 shows a rod that is attached to collinear semi-infinite rods of the same material but different cross-sectional area at each end. The

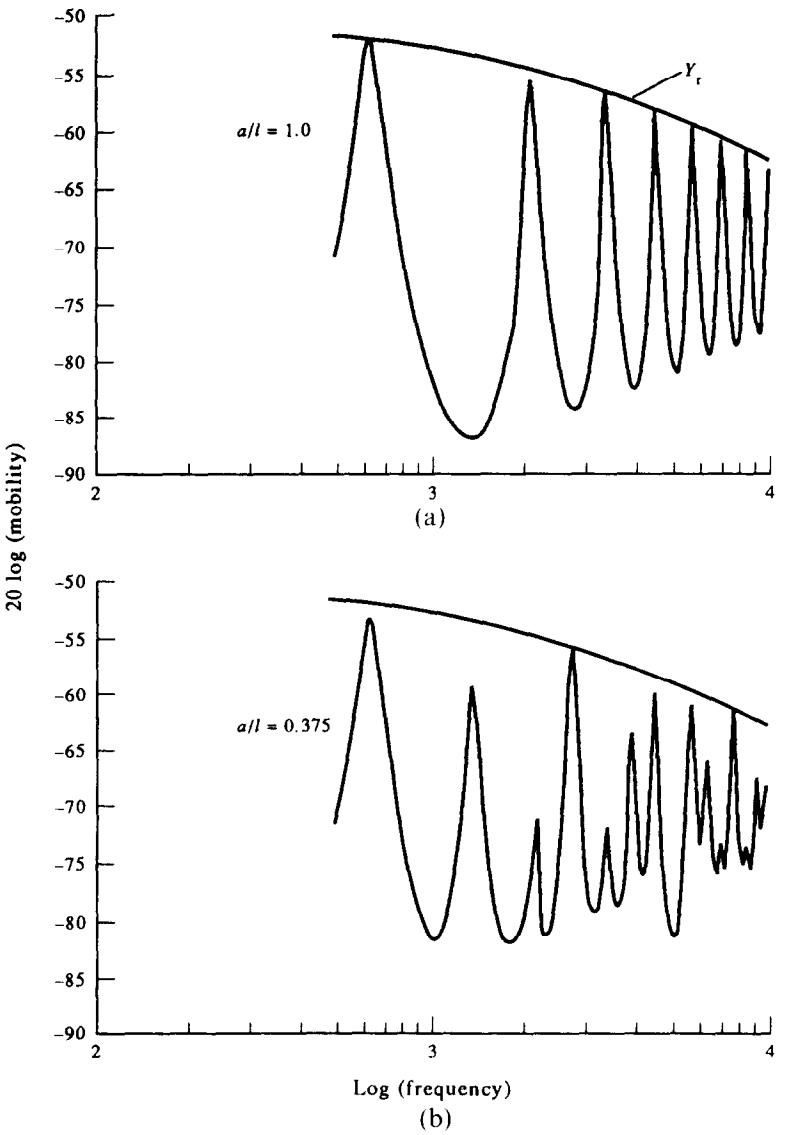


**Fig. 3.** Point mobility of a clamped rod for excitation at various positions.

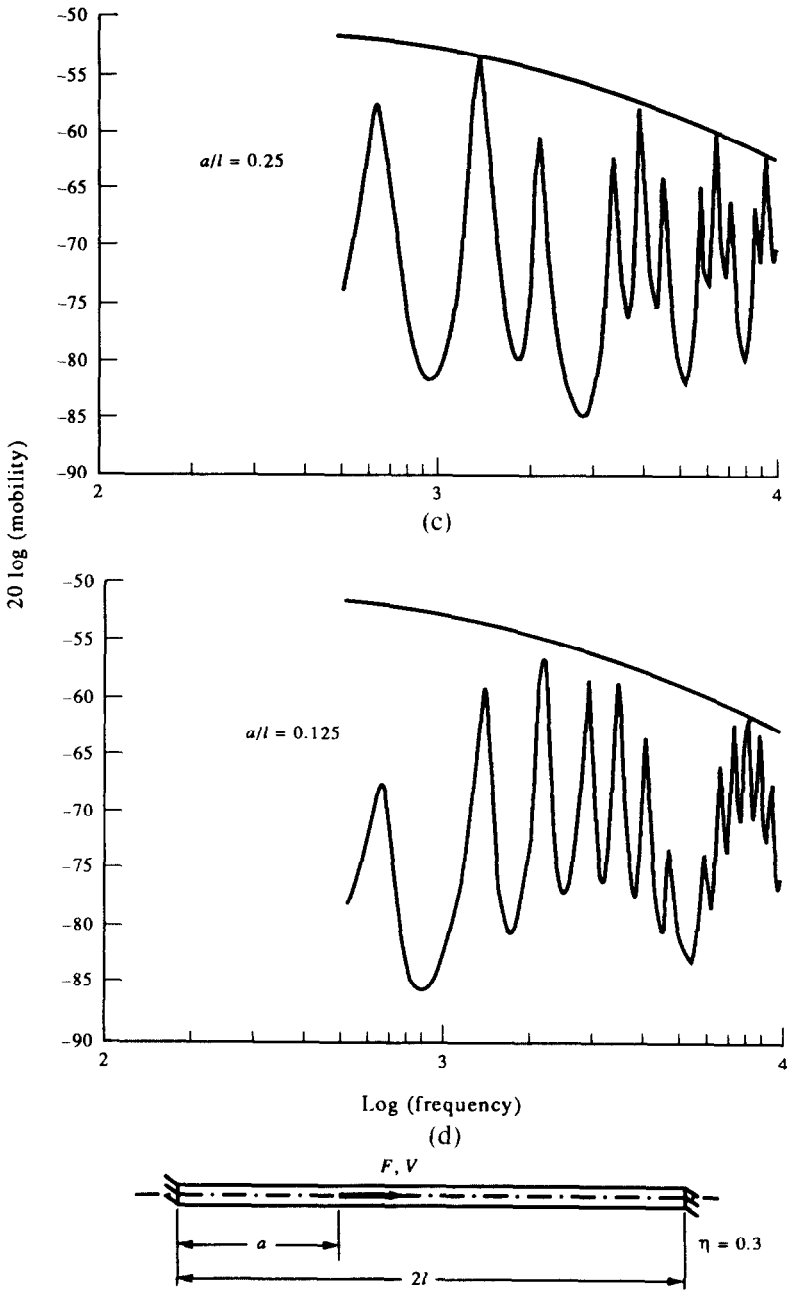
20 log (mobility)
-50
-55
-60
-65
-70
-75
-80
-85
-90
a/l = 0.25
2
3
4
(c)
a/l = 0.125
Log (frequency)
(d)
F, V
a
2l
η = 0.3

**Fig. 3**—*contd.*

efficiency of the coupling is dependent on the ratio of these areas $A_1$ and $A_2$; the transmission coefficient at the junction is given by:[5]

$$\tau = \frac{4A_1/A_2}{(A_1/A_2 + 1)^2} \tag{8}$$

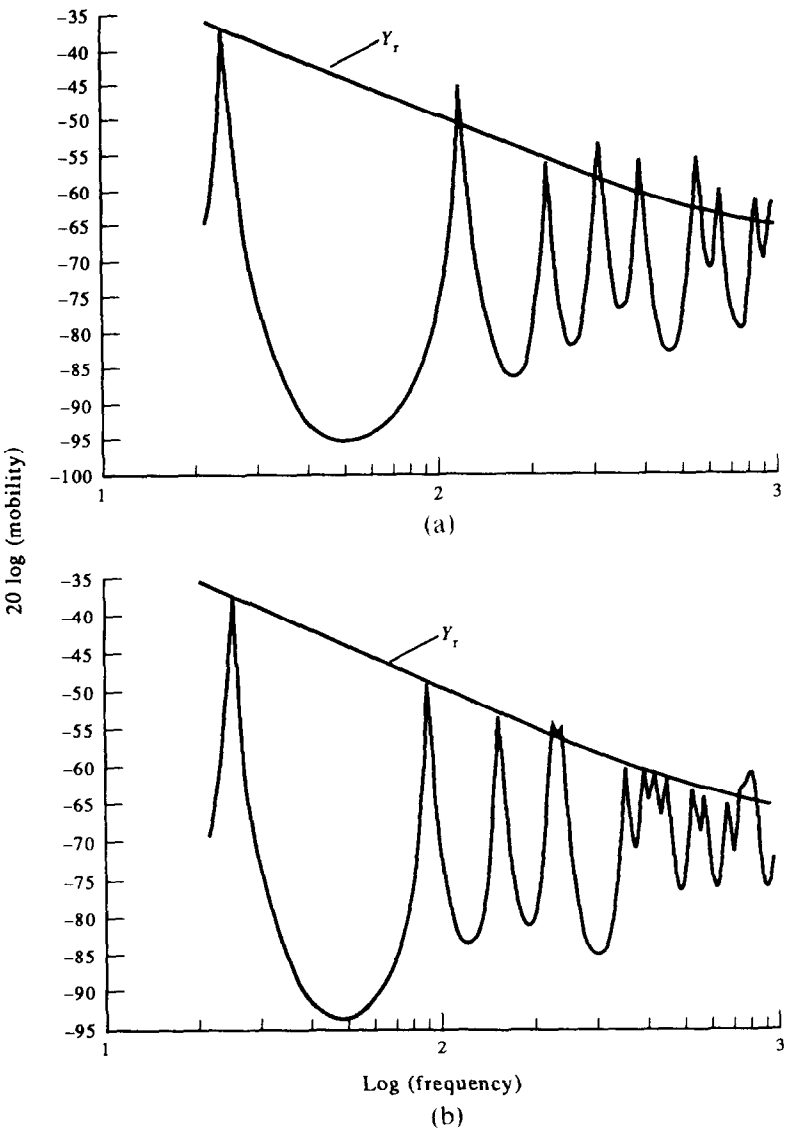


**Fig. 4.** Point mobility at the centre of simply supported plates of various aspect ratios. (a) Aspect ratio = 1; (b) aspect ratio = 1·36; (c) aspect ratio = 1·44; (d) aspect ratio = 1·5.

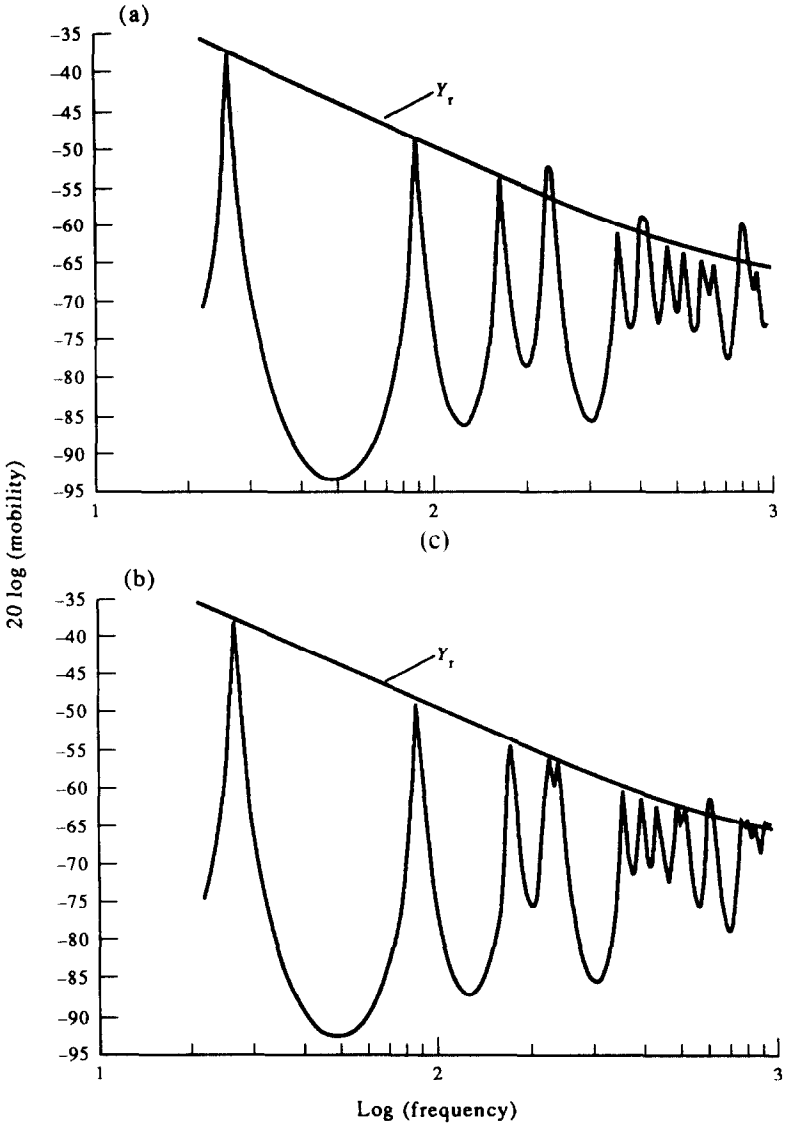


**Fig. 4**—*contd.*

Figure 5 shows the effect of these lossy boundary conditions. The height of the peaks decreases as energy is lost at the boundaries, as expected. In the limiting case where the coupling is perfect there are no reflections and the characteristic mobility is obtained.

Unfortunately, there is not complete agreement in the literature as to the correct definition of coupling loss factor. Sablik[14] gives three alternative definitions in common use:

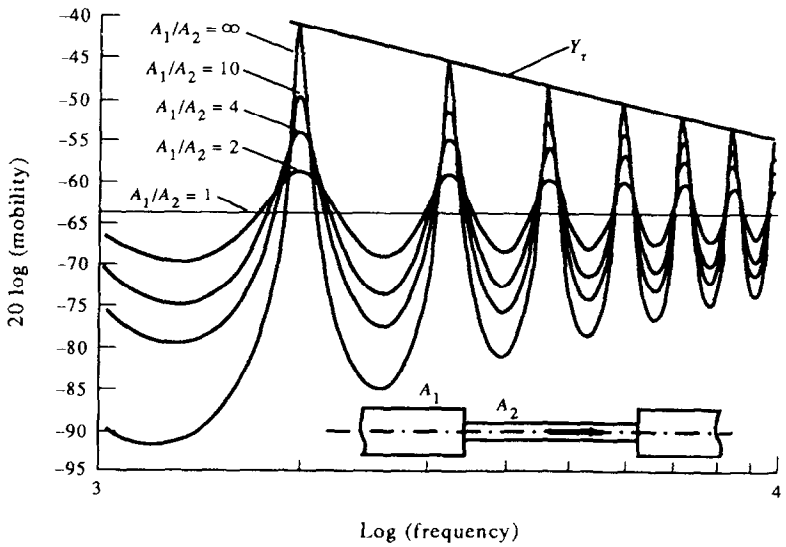


**Fig. 5.** Point mobility of a rod with various degrees of end loss.

$$\eta_c = \frac{c_L \cdot \tau}{l\omega} \tag{9}$$

$$\eta_c = \frac{c_L \cdot \tau}{2l\omega} \tag{10}$$

$$\eta_c = \frac{c_L \cdot \tau}{l\omega \cdot (2 - \tau)} \tag{11}$$

where $c_L$ is the longitudinal wave speed. The peak height has been predicted using each of these definitions and results, shown in Fig. 6, indicate reasonable agreement for definition (11), but eqn (9) is seen to be unconservative.

It can easily be shown that exact agreement would be obtained if $\eta_c$ were given by:

$$\eta_c = \frac{2c_L \cdot \tau}{l\omega \cdot [1 + \sqrt{(1 - \tau)}]^2} \tag{12}$$

and this represents an alternative definition of coupling loss factor which has been incidentally derived. It agrees closely with eqn (11) except at high values of $\tau$ unlikely to be encountered in practice. Definitions (9)–(11) have been derived on statistical bases, but Skudrzyk's theory,[1] which forms the basis of eqn (12), is exact, and it therefore seems likely that eqn (12) is

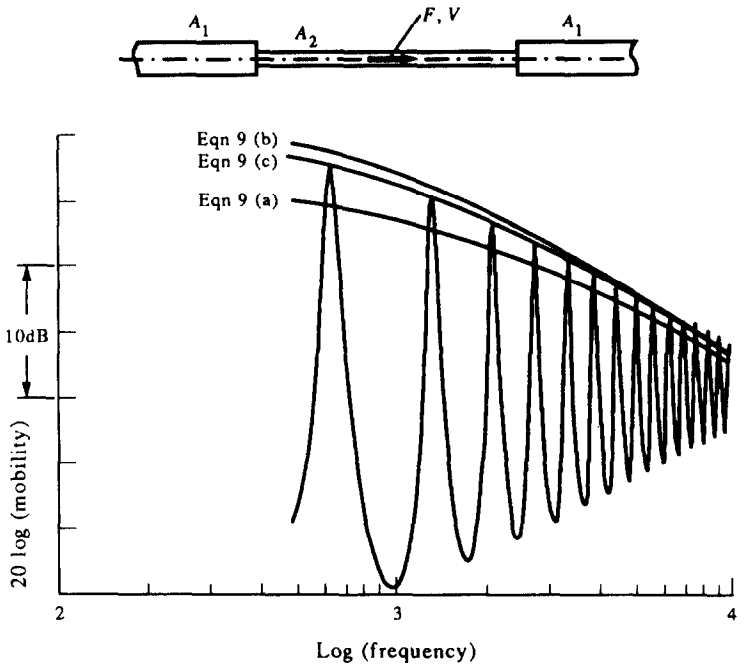


**Fig. 6.** Prediction of peak envelope using various definitions of coupling loss factor.

the correct definition. (Note that none of eqns (9)–(11) give $\beta \rightarrow 1$ which is the correct limit for $\tau \rightarrow 1$.)

It has thus been demonstrated that the upper bound is valid using the total loss factor in eqn (4) provided that the correct expression for coupling loss factor can be derived. When the receiving substructures are highly resonant this becomes difficult as coupling losses vary rapidly with frequency due to resonant behaviour. Consequently, the simplicity of the prediction is lost, although a conservative estimate is still possible, by assuming material losses only.

For beams, coupling losses are more appropriately described with an absorption coefficient:

$$\alpha = \sum_i \tau_i \tag{13}$$

where the $\tau_i$ are the transmission coefficients from the driven element to each of the receiver elements. Absorption coefficients for some common junctions are given in Fig. 7.

It is now possible to make predictions of the heights of the resonance peaks for beams using the absorption coefficient (Fig. 7), the definitions of coupling loss factor (eqns (9)–(11)) and eqn (4). These absorption

coefficients should be used with care since they are derived assuming all elements forming the junction are of identical materials and cross sections. Factors that cause an increase in impedance mismatch, such as a change in cross section or material, or poor joins between elements will tend to reduce the absorption coefficient, thereby increasing the height of the peaks.

For plates, the absorption coefficient depends on the angle of incidence of the incoming wave. Cremer[5] shows that the 'random incidence trans-

| Configuration | Normal incidence | Random incidence |
|---|---|---|
| 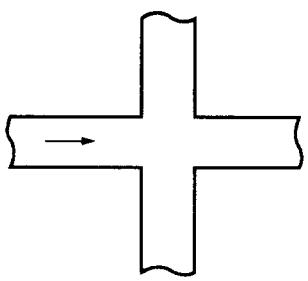 | 0.375 | 0.25 |
| 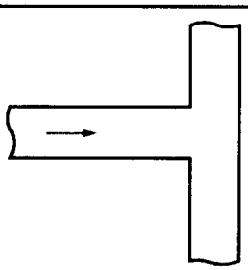 | 0.444 | 0.3 |
| 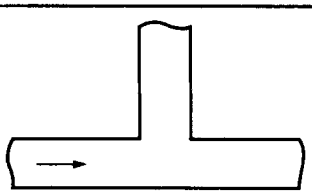 | 0.444 | 0.3 |
| 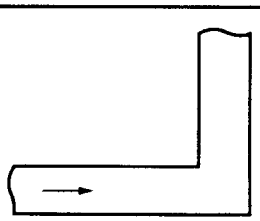 | 0.5 | 0.333 |

**Fig. 7.** Absorption coefficients for beam and plate junctions.

mission' coefficient is two-thirds of the normal incidence value. Transmission and absorption coefficients for plates are given in Fig. 7; as for beams, any change will cause a decrease in absorption coefficient. Craik[15] presents figures giving the absorption coefficients for all combinations of thickness and material properties, from which an absorption coefficient of 0·3 is seen to be reasonable for any configuration of similar plates, provided that the thicknesses do not vary by more than about 20%.

The coupling losses are given by Craik[15] as:

$$\eta_c = \frac{2}{\pi} \frac{1}{12(1-\nu^2|)} \sqrt{\frac{h \cdot c_L}{\omega}} \cdot \frac{U}{S} \cdot \bar{\alpha} \tag{14}$$

where $S$ is the area of the plate and $U$ the length of its perimeter. The mean absorption coefficient $\bar{\alpha}$ is defined as:

$$\bar{\alpha} = \frac{\sum_i l_i \alpha_i}{\sum_i l_i} \tag{15}$$

and the product $U\bar{\alpha}$ physically represents an equivalent length of perfectly absorbing boundary (analogous to Sabine's 'open window units' for room acoustics).

An expression for the heights of the peaks of plates with edge losses is obtained by combining equations (14) and (5), yielding:

$$Y_r = \frac{4{\cdot}56}{\rho U \bar{\alpha} h^{3/2} c_L^{1/2} f^{1/2}} \tag{16}$$

In eqn (16), it is assumed that material losses are dominated by edge losses, which is reasonable for most building structures and is in any case conservative. The peak envelope can be adjusted to account for overlapping modes by calculating the relative height of the peaks above the characteristic line, $\beta = Y_r / Y_c$, and then using eqn (6).

Equation (16) will now be tested against experimental results for concrete floors.

## 5 EXPERIMENTAL RESULTS FOR FLOORS

The measured point mobilities presented in Figs 8, 9 and 10 were obtained *in situ* by an impulse response method, in which the impulse is applied with a hammer and the response measured with an accelerometer. The pulse length was 2 ms for the measurements shown. Measurements were

made in the frequency range 0–1 kHz, thus covering most of the region of resonant behaviour. Prediction of the peak height was carried out according to eqn (16), and adjusted as described in section 4.

The floors were all concrete cast-in-situ type and therefore significant coupling losses were expected. It was assumed that fluctuations in the coupling losses due to resonances in the side walls would be minimal.

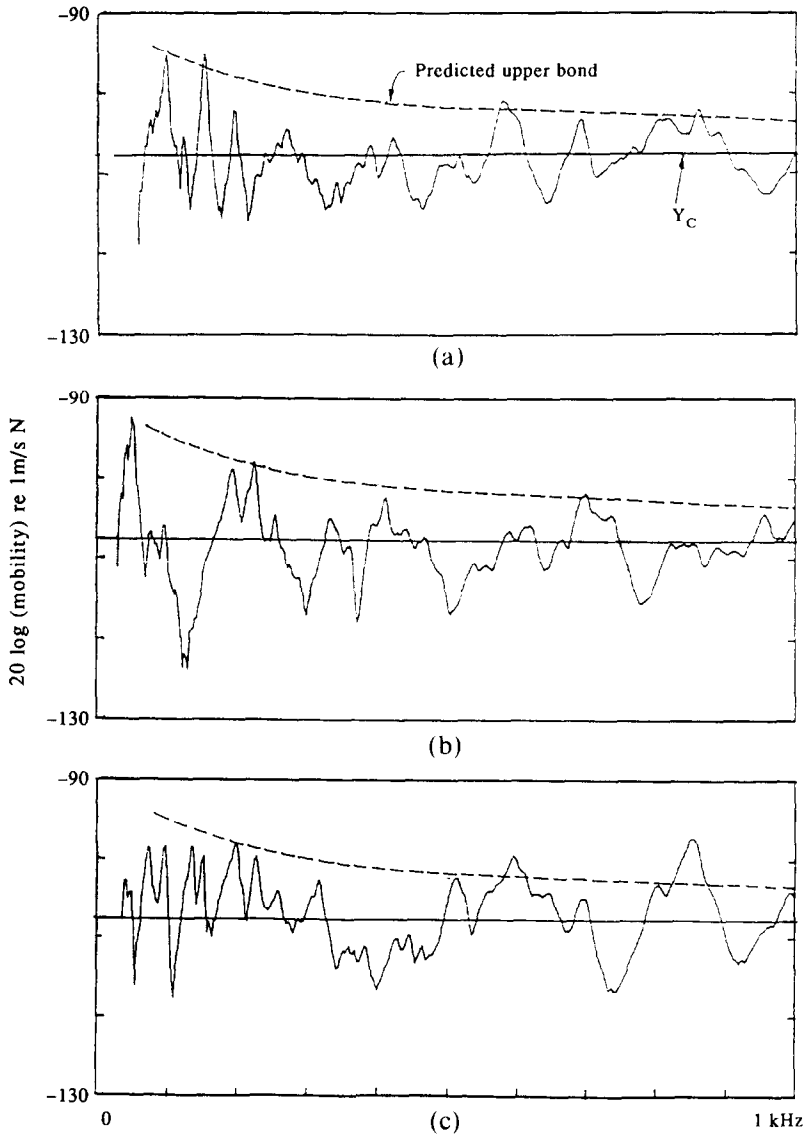


**Fig. 8.** Point mobility (real part) of the reverberation chamber. (a) Position A; (b) position E; (c) position G.

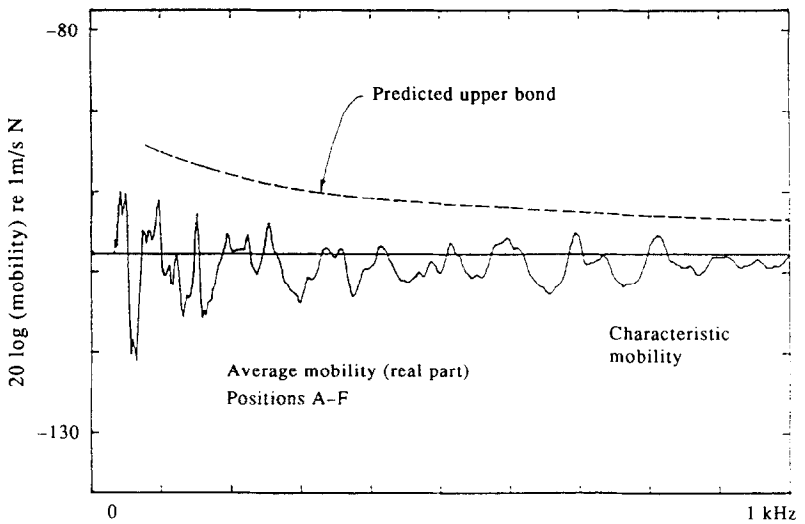


**Fig. 9.** Average of point mobility over positions A–F on reverberation chamber roof.

## 5.1 Roof of small reverberation chamber

The first example is the roof of a small reverberation chamber, shown in Fig. 11, which was of a typical concrete-slab construction. The 4·83 m × 3 m roof slab was of cast concrete 120 mm thick with a mass of 4·2 tonnes supported on brick walls 115 mm thick. The floor and wall plates formed right-angled junctions and an absorption coefficient of 0·33 is therefore appropriate from Fig. 7. The roof and walls were of different materials; however, brick and concrete have similar densities and Young's moduli so no allowance was thought necessary for this difference.

The measured point mobilities at the positions indicated are shown in Fig. 8. Results at all other positions are similar, with the worst agreement obtained for position G, thought to be due to imperfect joining between the floor and walls at this point. This may also have been a result of two coincident modes both being excited at antinodes at this position but this explanation would seem less likely. The results are encouraging, with the predicted mean and peak mobilities successfully characterising the measured curves.

When dealing with sources connected to the floor at multiple points the average of the mobilities at all connection points is of interest in determining structure-borne power into the floor.[3] Figure 9 shows the real part of mobility averaged over points A–F, which could be likened to the connection points for a typical machinery installation. The averaging

process has had the effect of reducing the variations about the mean value. This is because each resonance is excited to a different extent at each position.

## 5.2 Plant room floor

The plan and edge detailing of this plant room floor are shown in Fig. 12. The floor is of 300 mm concrete slab set into concrete walls at the edges.

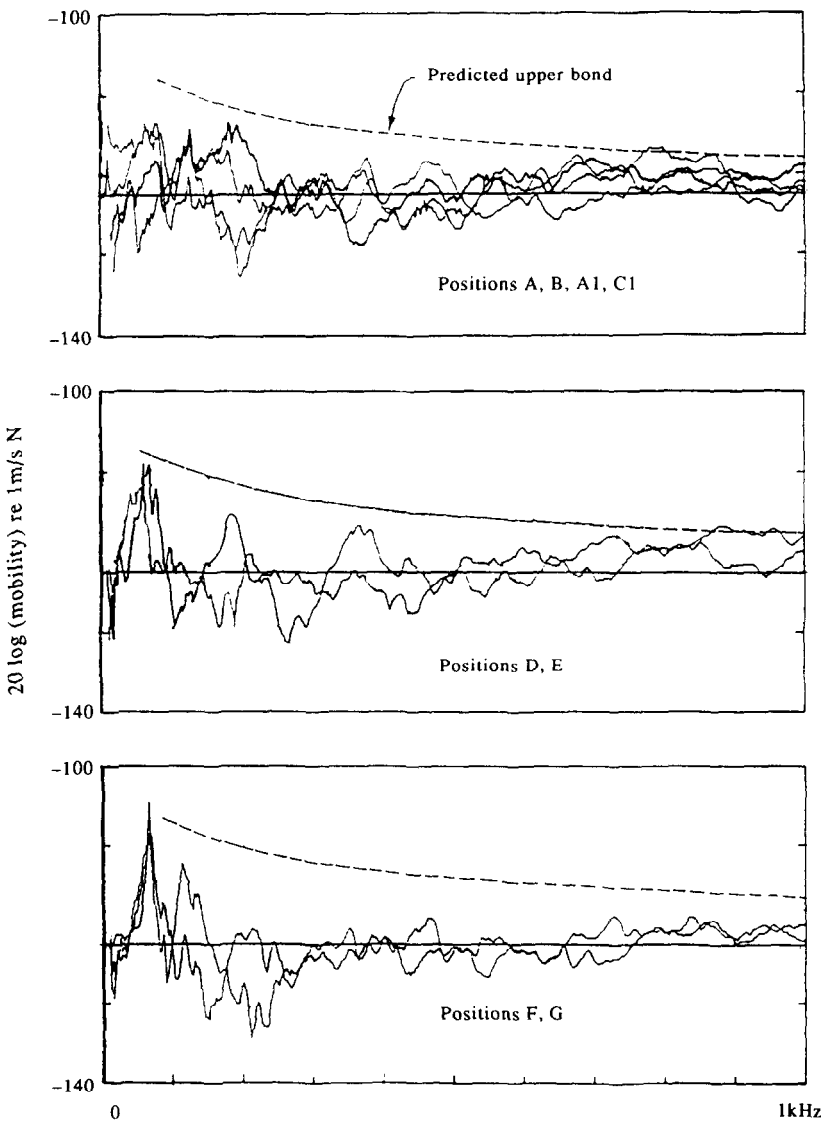


**Fig. 10.** Point mobility (real part) of the plant room floor.

One difficulty that immediately arises is that the floor is far from the rectangular shape assumed in the derivation of the theory. The plate has therefore been treated as two separate rectangular areas as shown. The absorption coefficient at the edges is variable depending on the ratio of floor to wall thickness, as shown in Fig. 12. Perfect reflection has been assumed at the riser cut-out and zero reflection at the open edge between the two areas. Mean absorption coefficients of 0·23 and 0·34 are applicable for the larger and smaller areas respectively.

The remaining results for the three sections are shown with the predictions in Fig. 10. As before, the characteristic mobility is a good approximation to the mean mobility up to 600 Hz, above which thick-plate theory is applicable,[16] and local stiffness causes an increase in mean mobility.

The predicted peak envelope is more conservative than in the previous example; this is possibly due to the floor having been split into two sections for the purpose of prediction, each with a lower mass than the whole floor.

Further measurements on a similar floor produced very similar results.

## 6 CONCLUDING REMARKS

It has been proposed to represent the mobility of concrete floors by a skeleton plot made up of the mean mobility and the envelope of the resonant peaks. The advantage of this simple characterisation is that the

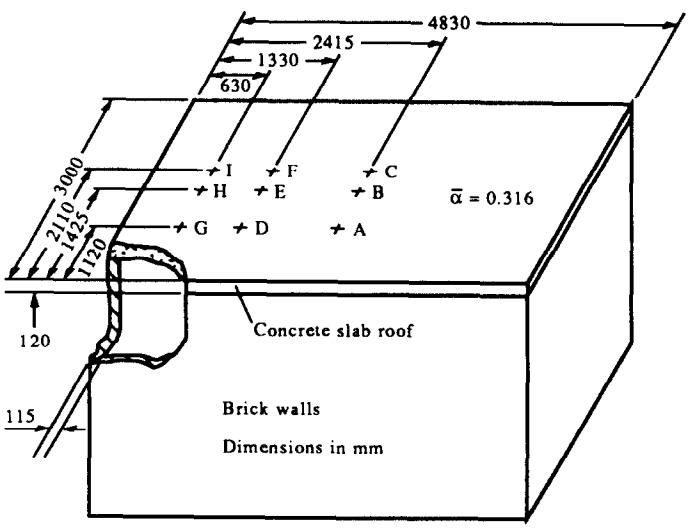


**Fig. 11.** The roof of the reverberation chamber.

essential features of the mobility plot can be established without a need for complex calculations. In particular, the natural frequencies of the floor need not be known because the envelope of the resonant peaks has been shown to be independent of the position of the actual resonances on the frequency plot.

An advantage of the above formulation over previous empirical methods is that it has a theoretical basis that yields insight into the problem. Empirical results cannot be extrapolated to new floor configurations, a particular difficulty being the influence of coupling losses. The above formulation allows the effect of losses at floor boundaries to be estimated.

The intended application is for prediction of structure-borne sound transmission through the contact points of machines installed in buildings, but the formulation is general.

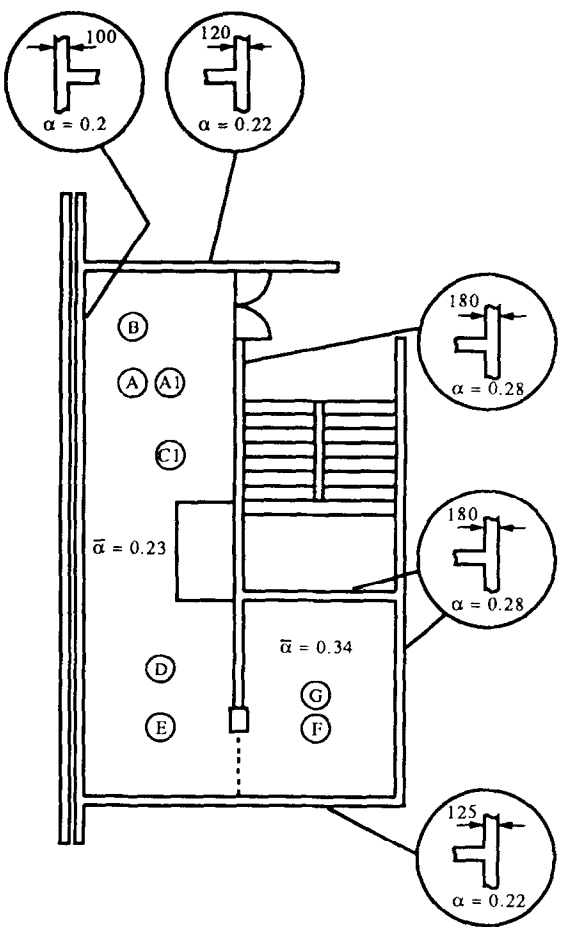


**Fig. 12.** Plan and edge detailing for plant room floor.

## ACKNOWLEDGEMENTS

The financial support of the Science and Engineering Research Council is gratefully acknowledged.

## REFERENCES

1. Skudrzyk, E., The mean value method of predicting the dynamic response of complex vibrators. *Journal of the Acoustic Society of America*, **67** (1981) 347–59.
2. Petersson, B. & Plunt, J., Structure-borne sound transmission from machinery to foundations. Report 80–19, Department of Building Acoustics, Chalmers University of Technology, Gothenburg, 1980.
3. Moorhouse, A. T. & Gibbs, B. M., Prediction of the structure-borne noise emission of machines: development of a methodology. *Journal of Sound and Vibration*, **167** (1993) 223–37.
4. Moorhouse, A. T. & Gibbs, B. M., Measurement of structure-borne sound emission from resiliently mounted machines in-situ. *Journal of Sound and Vibration*, (in press).
5. Cremer, L., Heckl, M. & Ungar, E. E., *Structure-Borne Sound.* Springer-Verlag, Berlin, 1973.
6. Melzig-Thiel, T. & Meltzer, G., Messung und Berechnung der Eingangs-admittanzen von Gebaudedecken. *Proceedings of 7th ICA Congress*, Budapest, 1971, pp. 577–80.
7. Breeuwer, R. & Tukker, J. C., Resilient mounting systems in buildings. *Applied Acoustics*, **9** (1976) 77–101.
8. Sho Kimura & Katsuo Inque, Practical calculation of floor impact sound by impedance method. *Applied Acoustics*, **26** (1989) 263–92.
9. Steel, J. A., Structure-borne sound in buildings at low frequencies. MSc thesis, Herriot-Watt University, Edingburgh, 1987.
10. Skudrzyk, E., Understanding the dynamic behaviour of complex vibrators. *Acustica*, **64** (1987) 123–47.
11. Williams, E., Vibrations of plates of various geometries. PhD thesis, Physics Department, Pennsylvania State University, 1980.
12. Petersson, B., An approximation for the point mobility at the intersection of two perpendicular plates. *Journal of Sound and Vibration*, **91** (1983) 219–38.
13. Hart, F. D. & Shah, K. C., Compendium of modal densities for structures. NASA Contractors Report CR-1773, 1971.
14. Sablik, M. J. *et al.* Statistical energy analysis, structural resonances and beam networks. *Journal of the Acoustic Society of America*, **77** (1985) 1038–45.
15. Craik, R. J. M., Damping of building structures. *Applied Acoustics*, **14** (1981) 347–59.
16. Heckl, M., Koerperschallubertragung bei homogonen Platten beliebiger Dicke. *Acustica* **49** (1981) 183–91.